

Suppression of phonon tunneling losses by microfiber strings for high-Q membrane microresonators

Zongyang Li,^{1,2} Qiang Zhang,^{1,2} Xiang You,^{1,2} Yongmin Li,^{1,2,a)} and Kunchi Peng^{1,2}

¹State Key Laboratory of Quantum Optics and Quantum Optics Devices, Institute of Opto-Electronics, Shanxi University, Taiyuan 030006, China

²Collaborative Innovation Center of Extreme Optics, Shanxi University, Taiyuan 030006, China

(Received 17 August 2016; accepted 27 October 2016; published online 8 November 2016)

We propose to utilize a microfiber string to isolate the tunneling of acoustic waves between a membrane frame and its holder. The displacement response of the membrane frame with and without the vibration isolation is characterized using an optical interferometer. A displacement power suppression of 40 dB is achieved around the fundamental mode frequency of the membrane. We demonstrate that the Q factor of a SiN membrane microresonator with our vibration isolation method can reach 1.78×10^6 in room temperature. *Published by AIP Publishing.*

[<http://dx.doi.org/10.1063/1.4967496>]

The highly stressed silicon nitride membranes with extraordinarily low optical absorption and mechanical dissipation properties have emerged as one of the most promising platforms in quantum optomechanics.¹⁻⁴ Recently, the mechanical modes of stoichiometric silicon nitride (Si₃N₄) membranes have been cooled to near the quantum ground state in the resolved sideband cooling regime.⁵⁻⁹ So far the Si₃N₄ membranes when operated in the so-called membrane-in-the-middle approach,³ have been employed for a number of impressed demonstrations of optomechanical experiments, such as the generation of optical nonclassical state,^{10,11} narrowing the filter-cavity bandwidth in gravitational-wave detectors,¹² and conversion between microwave and optical light.^{13,14} However, it should be noticed that the above mentioned experiments and other proposed protocols¹⁵⁻¹⁷ all require that the membrane resonators own a high mechanical Q factor.

The mechanical Q factor, which represents the dissipation of a resonator, can be divided into internal loss and external loss. The former one describes the energy loss inside the resonator which is dominated by the bending loss, while the latter one represents the energy loss outside of the resonator caused by the coupling between the resonator and its support structure, which is also called clamping loss, recoil losses, or tunneling loss.^{2,18-28} Previous studies show that the Q factor of a resonator can reach the upper bound which is dominated by the internal loss of the resonator if its external loss is well isolated. Although by elaborative design of the size, thickness, shape, and tensile stress of a membrane resonator, the bending loss can be reduced and the Q factor can reach more than 10^7 in room temperature,^{29,30} the clamping loss is still the most important limit factor for the effective mechanical Q that one can obtain in practice. At present, several approaches have been proposed to suppress the tunneling loss such as nodal suspension,²⁸ phononic crystal,²³⁻²⁵ and low frequency mechanical resonators.^{26,27,31,32} The phononic crystal technique is suitable for the vibration

isolation of relatively high frequency resonators since the size of its unit cell would be very large if a band gap centered at low frequency is required. The low frequency mechanical resonator approach which relies on the low pass filtering of mechanical vibration can be used in low frequency band isolation. For instance, suspending mirrors with silica fibers^{31,32} in the Gravitational wave detection system.

In this work, we present a simple and effective approach to suppress the acoustic waves between a membrane resonator and its surroundings with microstrings which consists of two tensioned microfibers. The isolation mechanism of the acoustic waves is attributed to both the mass-on-spring modes of the membrane frame plus the microstrings and the vibration modes of the microfibers. We characterize the mechanical response of the microfiber strings shielded membrane frame utilizing an optical interferometer. Up to 40 dB of vibration isolation from an external mechanical drive is achieved around the fundamental mode frequency of the membrane.

The sketch of our device is shown in Fig. 1(a) which consists of an aluminum holder, a SiN membrane deposited on a silicon chip, and a pair of tensioned microfiber strings. The diameter of the microfiber strings is on the order of several tens of micrometers which is sufficient to grasp the chip stably. With internal tension of several million Pascal, the microfiber strings are fixed onto the aluminum holder, and the membrane chip is then glued onto the fiber strings. In this way, the silicon chip plus the microfibers act as a low frequency resonator. Meanwhile, the microfiber sections between the membrane chip and the aluminum holder approximately form four doubly clamped microstrings.

In the low frequency range, the fiber string can be treated as a light spring and the silicon chip moves as a rigid body. In this case, the mechanical displacement response of the chip can be written as $\omega_0^2/(\omega_0^2 - \omega^2 - i\Gamma_0\omega)$, where ω_0 and Γ_0 are the resonant frequency and mechanical decay rate of the mass-on-spring mode, ω is the frequency of vibration. In the high frequency range, the resonant vibration of the fiber strings cannot be neglected, and the system should not be regarded as a single resonator but a coupled one. The

^{a)}Author to whom correspondence should be addressed. Electronic mail: yongmin@sxu.edu.cn.

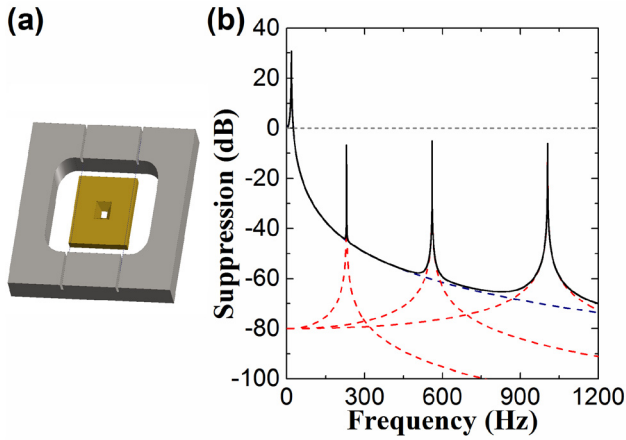


FIG. 1. (a) The microfiber strings shielded membrane resonator device which consists of an aluminum holder (gray), a SiN membrane chip (brown), and a pair of microfiber strings (dark blue). (b) Transfer function of the shielded device. The blue and red dashed lines denote the mass-on-spring mode of the silicon chip plus the microfibers and the microstrings mode, respectively. The black line is the overall transfer function considering both modes.

mechanical response of the silicon chip can be written as $m\omega_j^2/[M(\omega_j^2 - \omega^2 - i\Gamma_j\omega)]$, where ω_j and Γ_j are the resonant frequency and mechanical decay rate of the j th mode of the fiber string, m and M denote the mass of the fiber string and silicon chip, respectively. The theoretical vibration suppression of the device is shown in Fig. 1(b). Although the low frequency resonator can isolate the high frequency acoustic waves greatly. For instance, more than 60 dB isolation can be obtained given the low-frequency resonant frequency of 17 kHz and analysis frequency of above 400 kHz. The resonant vibration of the fiber strings themselves can degrade the isolation effect in the frequency range around their resonant frequencies and need to be considered. In order to tune the resonant frequencies of the microfiber strings to be away from the membrane modes and achieve a narrow resonance peak (high Q), the fiber diameter, length, and the tension should be carefully designed.

The eigenfrequencies of the square geometry high-stress membrane resonators can be written as $f_{mn} = \sqrt{\sigma(m^2 + n^2)/(4\rho l^2)}$, where $\sigma \approx 0.9$ GPa is the tensile stress, $\rho = 2.7$ g/cm³ is the density of silicon nitride, (m, n) are mode indices representing the number of antinodes, and $l = 500$ μ m is the side length of the square membrane. The frequencies of the (1, 1) and (2, 2) membrane modes can be calculated to be around 800 kHz and 1.6 MHz using above relation.

There are three types of vibration modes for a clamped fiber string, transverse mode (TM), longitudinal mode (LM), and radial breathing mode (RBM), as shown in Fig. 2. Since the vibration directions of LM and membrane mode are

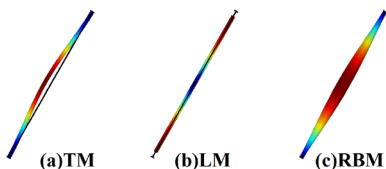


FIG. 2. Vibration modes of a doubly clamped fiber string. (a) transverse mode, (b) longitudinal mode, (c) radial breathing mode.

mutually perpendicular. The only type of vibration we need to pay attention to is the TM vibration (Fig. 2(b)). For a doubly clamped circular string under zero tension, the resonant frequency of the TM is given by³³

$$f_{0,n} = \frac{i_n^2}{2\pi L^2} \sqrt{\frac{YI}{\rho A}}, \quad (1)$$

where $Y = 73$ GPa and $\rho = 2.3$ g/cm³ are the Young modulus and density (silica), respectively, $I = \pi d^3/64$, and $A = \pi d^2/4$ are the moment of inertia and the cross sectional area of rounded strings, respectively, d is the diameter, L is the length, and i_n is the characteristic number for the n th mode, which are given by $i_1 = 4.73004$, $i_2 = 7.85320$, $i_3 = 10.99561$, and $i_n \approx (n+1)\pi/2$ for $n \geq 3$. When stress is applied to a string, the resonant frequency is increased according to the following equation:^{34,35}

$$f_n(\sigma) = f_{0,n} \sqrt{1 + 0.97 \frac{1}{(n+1)^2} \frac{\sigma A L^2}{YI}} \quad (2)$$

A thinner fiber string can lead to a better suppression of the vibration. On the other hand, according to Eq. (1), a thinner fiber string means that its resonant frequencies are lower, which results in dense resonant peaks of the fiber strings. To ensure wide spacing of the resonant peaks as well as good isolation of the vibration, the resonant frequencies should be improved without increasing the decay rate of the strings. To this end, we tense the fiber strings by hanging weight from the end of the strings during the assembling. This is due to the fact that the tension can increase the resonant frequency and tensile energy stored in the string, while keeping its energy decay intact.³⁶

The resonant frequencies of the first four modes of a silica microfiber (1-mm length and 30- μ m diameter) as a function of the applied load weights are shown in Fig. 3. It can be seen clearly that the resonant frequencies increase with the load weight applied to the strings. A 0.245 N weight which can generate 346.6 MPa tension inside the fiber string, is chosen in order to create the appropriate bandgap we need. In this case, the resonant frequencies of the first four modes

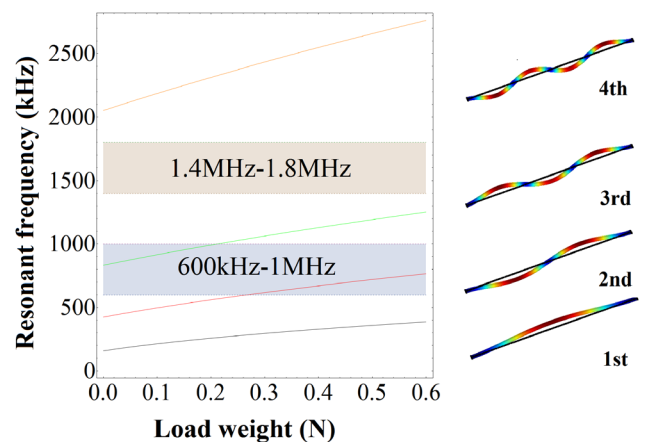


FIG. 3. Resonant frequencies of different vibration modes for a silica microfiber versus the applied load weight. Bandgap ranges are shown in grey and yellow.

are 275.3 kHz, 587.6 kHz, 1024.2 kHz, and 2368.9 kHz, respectively, which are well separated from the frequencies of the (1, 1) and (2, 2) membrane modes (800 kHz and 1.6 MHz).

The microfiber was fabricated through pulling 125- μm diameter single mode fibers to a diameter of 30 μm . The required stress inside the string was achieved by hanging weight from the end of the strings during the assembling. A three-dimension adjusting stage with a precision of 0.01 mm was exploited to put the silicon chip onto the fiber strings. The overall symmetry of the alignment is on the order of 5%. Start from the microfiber strings, we built a device as shown in Fig. 1(a) with a piezoelectric transducer fixed on the aluminum holder. Another membrane chip is also glued on the aluminum holder as a benchmark of the external mechanical drive. The mechanical response of the device is measured using an optical interferometer, i.e., a balanced-homodyne detector is used to probe the displacement spectra of the chip with and without the vibration isolation. To this end, a weak single frequency laser at 1064 nm is incident on the sample, and the reflected light is mixed with an intense local oscillator beam at a 50:50 beamsplitter. The relative phase between the signal light and the local oscillator is stabilized to $\pi/2$ to ensure the phase quadrature of the signal light that is measured. In order to avoid the influence of vibrations from the background environments, the sample is mounted on a stainless steel plate which is further installed on an anti-vibration rubber sheet. The output of a network analyzer is connected to the piezoelectric transducer to actuate the sample and the measured signal from the homodyne detector, which is in turn fed into the network analyzer.

Fig. 4 plots the measured mechanical response of the device. The observed resonant peaks of the membrane chip are attributed to the resonant response of the silicon substrate modes and the fiber strings. The resonant frequencies of the first three modes of the fiber strings (273.8 kHz, 576 kHz, and 1025 kHz) are marked with vertical dashed lines. An average of 30 dB vibration suppression can be observed from 200 kHz to 1.9 MHz, and it can reach up to 40 dB in the frequency band from 200 kHz to 1 MHz.

Finally, the mechanical Q of the SiN membrane for (1, 1) and (2, 2) modes is characterized using a mechanical

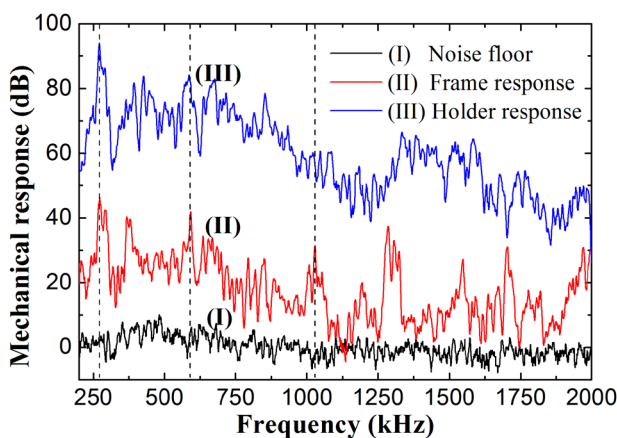


FIG. 4. (a) The mechanical response spectra. (I) Noise floor of the balanced homodyne detector; (II) Displacement power spectra of the membrane frame; (III) Displacement power spectra of the aluminum holder.

ringdown technique. The Q factor is defined as $Q_m = 2\pi f\tau$, where f is the center frequency of mechanical modes and τ is the ringdown time of mechanical energy. A typical result is shown in Fig. 5, the measured Q value can reach 1.78×10^6 for the fundamental mode and 1.56×10^6 for the (2, 2) mode at room temperature and a vacuum pressure of 8×10^{-6} mbar. Fig. 5(b) plots the displacement power spectra of the (2, 2) mode which is measured with a spectrum analyzer and the absence of external driving power. The observed linewidth of $\Gamma = 1$ Hz is limited by the resolution bandwidth (1 Hz) of the spectrum analyzer. Inserting the value of linewidth Γ into $Q_m = f/\Gamma$, the Q value is derived to be 1.52×10^6 . The quality factor from the direct spectrum measurement is in good agreement with the result of the ringdown detection.

In conclusion, we have provided a simple and cost-effective approach method to suppress efficiently the transmission of acoustic waves with microfiber strings. In this way, the phonon tunneling loss of the SiN membrane modes to the environment is effectively eliminated. The Q factors of both (1, 1) and (2, 2) modes are enhanced to be more than one and half a million in room temperature. The method we proposed enables the realization of high quality factor membrane resonators based on off-the-shelf membrane device. In future work, to avoid the use of glue, one can try to weld the fiber string onto the membrane frame with a laser welding,

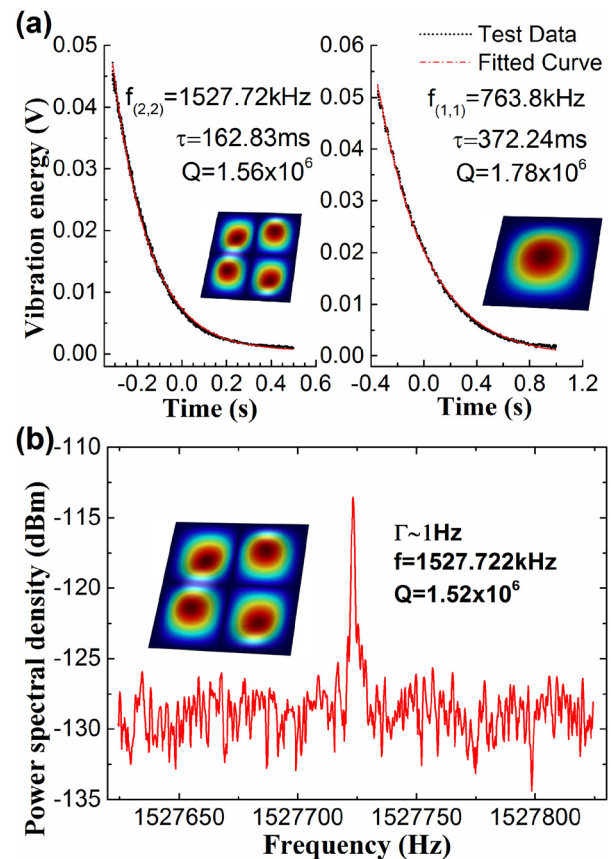


FIG. 5. (a) The quality factors of the fundamental mode and (2, 2) mode for a microfiber string isolated SiN membrane device using ringdown measurements. The data are fitted by exponential decay and the vibration ringdown time is 372.2 ms and 162.8 ms, respectively. (b) Power spectrum of the (2, 2) mode. The 1 Hz linewidth observed is subjected to the resolution bandwidth of the spectrum analyzer (1 Hz).

or fabricate the strings monolithically with the membrane frame using etching. It is noted that³⁷ by designing phononic crystal inside the membrane, both internal and external loss have been reduced significantly and the mechanical $Q > 10^8$ can be observed at room temperature.

This research was supported by the National Natural Science Foundation of China (NSFC) (61378010), the Key Project of the Ministry of Science and Technology of China (2016YFA0301403), the Natural Science Foundation of Shanxi Province (2014011007-1), and the Program for the Outstanding Innovative Teams of Higher Learning Institutions of Shanxi.

- ¹M. Aspelmeyer, T. J. Kippenberg, and F. Marquardt, *Rev. Mod. Phys.* **86**, 1391 (2014).
- ²D. J. Wilson, C. A. Regal, S. B. Papp, and H. J. Kimble, *Phys. Rev. Lett.* **103**, 207204 (2009).
- ³J. D. Thompson, B. M. Zwickl, A. M. Jayich, Florian Marquardt, S. M. Girvin, and J. G. E. Harris, *Nature* **452**, 72 (2008).
- ⁴T. P. Purdy, R. W. Peterson, and C. A. Regal, *Science* **339**, 801 (2013).
- ⁵M. Underwood, D. Mason, D. Lee, H. Xu, L. Jiang, A. B. Shkarin, K. Børkje, S. M. Girvin, and J. G. E. Harris, *Phys. Rev. A* **92**, 061801 (R) (2015).
- ⁶T. P. Purdy, R. W. Peterson, P. L. Yu, and C. A. Regal, *New J. Phys.* **14**, 115021 (2012).
- ⁷M. Karuza, C. Molinelli, M. Galassi, C. Biancofiore, R. Natali, P. Tombesi, G. D. Giuseppe, and D. Vitali, *New J. Phys.* **14**, 095015 (2012).
- ⁸R. W. Peterson, T. P. Purdy, N. S. Kampel, R. W. Andrews, P. L. Yu, K. W. Lehnert, and C. A. Regal, *Phys. Rev. Lett.* **116**, 063601 (2016).
- ⁹A. M. Jayich, J. C. Sankey, K. Børkje, D. Lee, C. Yang, M. Underwood, L. Childress, A. Petrenko, S. M. Girvin, and J. G. E. Harris, *New J. Phys.* **14**, 115018 (2012).
- ¹⁰T. P. Purdy, P. L. Yu, R. W. Peterson, N. S. Kampel, and C. A. Regal, *Phys. Rev. X* **3**, 031012 (2013).
- ¹¹W. H. P. Nielsen, Y. Tsaturyan, C. B. Meller, E. S. Polzik, and A. Schliesser, "Multimode optomechanical system in the quantum regime," e-print [arXiv:1605.06541v1](https://arxiv.org/abs/1605.06541v1).
- ¹²Y. Ma, S. L. Danilishin, C. Zhao, H. Miao, W. Z. Korth, Y. Chen, R. L. Ward, and D. G. Blair, *Phys. Rev. Lett.* **113**, 151102 (2014).
- ¹³R. W. Andrews, R. W. Peterson, T. P. Purdy, K. Cicak, R. W. Simmonds, C. A. Regal, and K. W. Lehnert, *Nat. Phys.* **10**, 321 (2014).
- ¹⁴T. Bagci, A. C. Simonsen, S. Schmid, E. Zeuthen, J. Appel, J. M. Taylor, A. Sørensen, K. Usami, A. Schliesser, and E. S. Polzik, *Nature* **507**, 81 (2014).
- ¹⁵M. Karuza, C. Biancofiore, M. Bawaj, C. Molinelli, M. Galassi, R. Natali, P. Tombesi, G. D. Giuseppe, and D. Vitali, *Phys. Rev. A* **88**, 013804 (2013).
- ¹⁶S. Schmid, T. Bagci, E. Zeuthen, J. M. Taylor, P. K. Herring, M. C. Cassidy, C. M. Marcus, L. G. Villanueva, B. Amato, A. Boisen, Y. C. Shin, J. Kong, A. S. Sørensen, K. Usami, and E. S. Polzik, *J. Appl. Phys.* **115**, 054513 (2014).
- ¹⁷A. B. Shkarin, N. E. Flowers-Jacobs, S. W. Hoch, A. D. Kashkanova, C. Deutsch, J. Reichel, and J. G. E. Harris, *Phys. Rev. Lett.* **112**, 013602 (2014).
- ¹⁸P.-L. Yu, T. P. Purdy, and C. A. Regal, *Phys. Rev. Lett.* **108**, 083603 (2012).
- ¹⁹I. Wilson-Rae, R. A. Barton, S. S. Verbridge, D. R. Southworth, B. Ilic, H. G. Craighead, and J. M. Parpia, *Phys. Rev. Lett.* **106**, 047205 (2011).
- ²⁰S. Chakram, Y. S. Patil, L. Chang, and M. Vengalattore, *Phys. Rev. Lett.* **112**, 127201 (2014).
- ²¹A. Jöckel, M. T. Rakher, M. Korppi, S. Camerer, D. Hunger, M. Mader, and P. Treutlein, *Appl. Phys. Lett.* **99**, 143109 (2011).
- ²²K. K. Ni, R. Norte, D. J. Wilson, J. D. Hood, D. E. Chang, O. Painter, and H. J. Kimble, *Phys. Rev. Lett.* **108**, 214302 (2012).
- ²³A. H. Safavi-Naeini and O. Painter, *Opt. Express* **18**, 14926 (2010).
- ²⁴Y. Tsaturyan, A. Barg, A. Simonsen, L. G. Villanueva, S. Schmid, A. Schliesser, and E. S. Polzik, *Opt. Express* **22**, 6810 (2014).
- ²⁵P.-L. Yu, K. Cicak, N. S. Kampel, Y. Tsaturyan, T. P. Purdy, R. W. Simmonds, and C. A. Regal, *Appl. Phys. Lett.* **104**, 023510 (2014).
- ²⁶A. Borrielli, L. Marconi, F. Marin, F. Marino, B. Morana, G. Pandraud, A. Pontin, G. A. Prodi, P. M. Sarro, E. Serra, and M. Bonaldi, *Phys. Rev. B* **94**, 121403(R) (2016).
- ²⁷M. J. Weaver, B. Pepper, F. Luna, F. M. Buters, H. J. Eerks, G. Welker, B. Perock, K. Heeck, S. de Man, and D. Bouwmeester, *Appl. Phys. Lett.* **108**, 033501 (2016).
- ²⁸G. D. Cole, I. Wilson-Rae, K. Werbach, M. R. Vanner, and M. Aspelmeyer, *Nat. Commun.* **2**, 231 (2011).
- ²⁹R. A. Norte, J. P. Moura, and S. Gröblacher, *Phys. Rev. Lett.* **116**, 147202 (2016).
- ³⁰C. Reinhardt, T. Müller, A. Bourassa, and J. C. Sankey, *Phys. Rev. X* **6**, 021001 (2016).
- ³¹N. A. Robertson, G. Cagnoli, D. R. M. Crooks *et al.*, *Classical Quantum Gravity* **19**, 4043 (2002).
- ³²M. Lorenzini on behalf of Virgo Collaboration, *Classical Quantum Gravity* **27**, 084021 (2010).
- ³³D. Young and R. P. Felgar, Jr., *Tables of Characteristic Functions Representing Normal Modes of Vibration of a Beam* (The University of Texas, 1949), p. 12.
- ³⁴A. Bokaian, *J. Sound Vib.* **142**, 481 (1990).
- ³⁵S.-C. Jun, X. M. H. Huang, M. Manolidis, C. A. Zorman, M. Mehregany, and J. Hone, *Nanotechnology* **17**, 1506 (2006).
- ³⁶S. Schmid, K. D. Jensen, K. H. Nielsen, and A. Boisen, *Phys. Rev. B* **84**, 165307 (2011).
- ³⁷Y. Tsaturyan, A. Brag, E. S. Polzik, and A. Schliesser, "Ultra-coherent nanomechanical resonators via soft clamping and dissipation dilution," e-print [arXiv:1608.00937v1](https://arxiv.org/abs/1608.00937v1).